Available online at www.sciencedirect.com
ScienceDirect
Journal of Solid State Chemistry 180 (2007) 2–7
JOURNAL OF SOLID STATE CHEMISTRY
www.elsevier.com/locate/jssc

Crystal-structure and Mössbauer studies of $Li_{1.746}Nd_{4.494}FeO_{9.493}$

Miha Drofenik[a,b,*], Irena Ban[a], Darko Makovec[b], Darko Hanžel[b], Amalija Golobič[c], Ljubo Golič[c]

[a]*Faculty of Chemistry and Chemical Engineering, University of Maribor, Smetanova 17, SI-2000 Maribor, Slovenia*
[b]*"Jožef Stefan" Institute, Ljubljana, Slovenia*
[c]*University of Ljubljana, Faculty of Chemistry and Chemical Technology, Ljubljana, Slovenia*

Received 12 April 2006; received in revised form 3 August 2006; accepted 12 August 2006
Available online 1 September 2006

Abstract

The $Li_{1.746}Nd_{4.494}FeO_{9.493}$ (LNF) ternary phase, located in the Li_2O-rich part of the Li_2O–Nd_2O_3–Fe_2O_3 system, crystallizes with a cubic unit cell of dimension $a = 11.9763(3)$ Å and the space group $Im3m$. Refinement on F resulted in $R = 1.9\%$. The structure is comprised of a network of corners, edges and faces sharing the coordination polyhedra of neodymium. In between this skeleton the regular octahedra of oxygen-coordinated iron and trigonal prisms of lithium are located. The Mössbauer spectra revealed the presence of Fe^{3+}, Fe^{4+} and Fe^{5+} ions distributed on two symmetry-independent lattice positions.

Keywords: Crystal structure; Ternary compound; Single-crystal X-ray diffraction; Mössbauer spectroscopy; Iron oxidation state

1. Introduction

In a recent paper [1] the subsolidus equilibrium of Li–Nd–Fe–O was reported; this is isostructural with the ternary phase system Li–La–Fe–O studied in the 1980s by various authors [2–4]. The main aim of these investigations was to study the crystal structure of the only ternary phase identified in this ternary system, which has the general formula $LnLi_{1.5}Men^{+}{}_xO_{1.75+0.5nx}$, where *Ln* is La or Nd, and Me is Pt, Ti, Fe, Cr, or Ga [5].

In spite of the intensive investigations of this ternary phase in the past [5], these studies did not offer enough evidence of its constitution and structure. In this contribution the crystal structure of the ternary phase LNF was studied using X-ray structure analysis and Mössbauer spectroscopy.

The basic network of the structure remains the same, but as computing power and X-ray diffraction instrumentation has evolved, more details are emerging about the structure. For a detailed discussion of previous structural investigations the reader is referred to Refs. [2–4].

2. Experimental work

For the investigation of this structure single crystals were grown using Li_2CO_3 as a melt. The starting oxides used for preparing the samples were Nd_2O_3 (Ventron 99.9%), Li_2CO_3 (Ventron 99.8%) and Fe_2O_3 (Alfa product 99.8%).

The raw powders Nd_2O_3, Li_2CO_3, and Fe_2O_3 were weighed in accordance with the ternary composition $Li_5Nd_4FeO_{10}$ found during the investigation of the subsolidus phase diagram [1] and calcined at 1000 °C. The powder diffraction pattern of the calcined mixture was identical to the ternary phase reported in Ref. [1]. This synthesized phase $Li_5Nd_4FeO_{10}$ was admixed with 70 wt% Li_2CO_3 and heated at 760 °C for 2 weeks in a gold crucible. The crystals were leached out from the crucible with water, alcohol and dilute acetic acid. The XRD of the powdered samples shows only a diffraction pattern consistent with LNF. An inspection of the sample with an optical microscope revealed that the crystals obtained were in the form of regular black polyhedra with a size of about 0.1–0.01 mm. Many of them were grown together;

*Corresponding author. Faculty of Chemistry and Chemical Engineering, University of Maribor, Smetanova 17, SI-2000 Maribor, Slovenia. Fax: +386 1 4773 875.
E-mail addresses: miha.drofenik@uni-mb.si, miha.drofenik@ijs.si (M. Drofenik).

0022-4596/$ - see front matter © 2006 Elsevier Inc. All rights reserved.
doi:10.1016/j.jssc.2006.08.029

however, enough of them were suitable for the single-crystal X-ray diffraction analysis. A thorough inspection of the sample indicated the presence of some impurities. The EDX analysis showed that these white crystals were Nd_2O_3. However, the number of these crystals was small and did not significantly influence the measurements of the density or the chemical composition. The density of the crystallites was measured using Archimedes' method and a hexane picnometer and was $D_m = 6.74(5)\,g/cm^3$. Chemical analysis (ICP-AS) was used to determine the chemical composition of the crystals. These crystals were found to have a chemical composition of $Li_{2.22}Nd_{5,93}FeO_{11.49}$, where the iron was assumed to be in the 3+ state only. The absorber for the Mössbauer measurements was prepared from ground LNF single crystals, mixed with BN and put into a sample holder. The source was ^{57}Co in rhodium, and the spectra were measured at room temperature and at 77 K with a constant acceleration spectrometer. The velocity scale was calibrated with a 25-μm-thick metallic iron foil. The spectra were fitted with Lorentzian lines.

The unit-cell parameters were determined from the least-squares refinement of 376 reflections in the range $\theta = 1.02-27.48^\circ$ (MoK_α radiation). Additional data-collection parameters and crystallographic details are given in Table 1.

Bond valence sums, as outlined by Brese and O'Keeffe [6], were calculated for refinements where the site occupancies of the Fe atoms were refined. The valence of the bond between the iron atoms and the oxygen was estimated by $v_{ij} = \exp[(R_{ij}—d_{ij})/b]$, where d_{ij} is the bond length, b is a constant equal to 0.37 Å and R_{ij} is the bond-valence parameter from Ref. [7]. The bond-valence sum is given by $V_{ij} = \Sigma_j v_{ij}$ and should be approximately equal to the valence of the cation examined.

The structure was solved by a process of trial and error. A full-matrix least-squares refinement on F of all the atoms with anisotropic displacement parameters and an empirical weighting scheme, $w = 2.4 w_f w_s$, $w_f(F_o < 218.0) = (F_o/218.0)^{1.5}$, $w_f(F_o > 220.0) = (220.0/F_o)^2$, $w_f(218.0 < F_o < 220.0) = 1.0$, $w_s(\sin\theta/\lambda < 0.50) = ((\sin\theta/\lambda)/0.50)^4$, $w_s(\sin\theta/\lambda > 0.51) = (0.51/(\sin\theta/\lambda))^8$, $w_s(0.50 < \sin\theta/\lambda < 0.51) = 1.0$, was applied.

The *Xtal3.72* system of crystallographic programs [9] was used for the reduction of the data, the structure refinement and the interpretation. The graphic representation was produced using the ATOMS program [10]. Further details of the crystal data, the data collection and the refinement can be found in Table 1. Detailed crystallographic data have been deposited with the Fachinformationszentrum Karlsruhe (FIZ), D-76344 Eiggenstein-Leopoldshafen, with the deposition number CSD 415957.

The refined fractional coordinates and the equivalent isotropic thermal parameters and site occupancies are given in Table 2, and the refined cation-oxygen bond lengths, the calculated average bond lengths are given in Table 3. The results reported in Tables 2 and 3 reflect the refinement where the site occupancies of the atoms were refined.

3. Results and discussion

3.1. The structure description

The position of the neodymium, lithium, iron and oxygen atoms on the different independent positions of the space group *Im*3*m* are given in Table 2. The formula per unit cell calculated after the refinements of the site occupancies is $Li_{13.98}Nd_{36.00}Fe_{8.01}O_{76.04}$ ($Li_{1.746}Nd_{4.494}FeO_{9.493}$). The neodymium atoms occupy two symmetry-independent positions, Nd(1) with multiplicity 24 and

Table 1
Crystal data, data collection and refinement summary

Crystal data	Data collection	Refinement
$Li_{1.746}Nd_{4.494}FeO_{9.493}$	Nonius KAPPA CCD	Refinement on F
$M_r = 867.981$	ω scans	$R = 0.019$
Cubic, *Im*3*m*	Absorption correction: multi-scan(DENSO-SMN)	w$R = 0.0068$
$a = 11.9763(3)$ Å		$S = 1.013$
$V = 1717.78(7)$ Å^3	3201 measured reflections	217 reflections
$Z = 8$	224 independent	30 parameters
$D_m = 6.74(5)\,g/cm^3$	Reflections	w = empirical
$D_x = 6.721\,g/cm^3$	217 reflections with	Extinction correction:
MoK_α radiation	$I > 2.5\sigma(I)$	Zachariasen
Cell parameters from 376 reflections	$R_{int} = 0.037$	Extinction coefficient:
	$\theta_{max} = 27.48^\circ$	0.04872(464) [8]
$\theta = 1.02-27.48^\circ$	$h = -15 \rightarrow 15$	$(\Delta/\sigma)_{max} = 0.005849$
$\mu = 28.387\,mm^{-1}$	$k = -10 \rightarrow 10$	$(\Delta/\sigma)_{aver} = 0.000426$
	$l = -10 \rightarrow 10$	$\Delta\rho_{max} = 1.5\,eÅ^{-3}$
$T = 293(2)$ K		$\Delta\rho_{min} = -3.0\,eÅ^{-3}$
Block, black		
$0.06 \times 0.05 \times 0.04$ mm		
$0.182 < T < 0.242$		

Table 2
Fractional coordinates, equivalent displacement parameters (Å^2) and occupation parameters. U_{eq} is defined as one-third of the trace of the orthogonalized U_{ij} tensor

	x/a	y/b	z/c	U_{eq}	PP
Nd(1)	0	0.30714(1)	0.30714(1)	0.0087(2)	1.000
Nd(2)	0.34804(3)	0	0	0.0051(2)	1.000
Fe(1)	0	0	0	0.0054(4)	0.965
Fe(2)	0.25	0.25	0.25	0.0028(3)	0.760
O(1)	0	0.1522(5)	0	0.031(3)	0.749
O(2)	0.3622(1)	0.3622(1)	0.1925(2)	0.0119(9)	0.988
O(3)	0.25	0.5	0	0.017(3)	0.520
O(4)	0.1316(4)	0.5	0	0.013(2)	0.558
Li	0.1281(6)	0.1281(6)	0.1281(6)	0.017(2)	0.874

Table 3
Bond distances and bond angles with e.s.d.s in parentheses

Bond distances (Å)		Bond distances (Å)	
2 × Nd(1)–O(3)	2.4090(3)	Nd(2)–O(1)	2.345(7)
2 × Nd(1)–O(4)	2.423(2)	4 × Nd(2)–O(2)	2.385(2)
2 × Nd(1)–O(2)	2.487(2)	4 × Nd(2)–O(4)	2.407(3)
4 × Nd(1)–O(2	2.615(2)	3 × Li–O(1)	2.188(7)
6 × Fe(1)–O(1)	1.823(7)	3 × Li–O(2)	2.155(7)
6 × Fe(2)–O(2)	2.021(2)		

Bond angles (°)		Bond angles (°)	
O(3)–Nd(1)–O(3)	123.010(6)	O(1)–Fe(1)–O(1)	180.000
O(3)–Nd(1)–O(4)	88.9(1)	O(1)–Fe(1)–O(1)	90.000
O(3)–Nd(1)–O(4)	34.1(1)	O(2)–Fe(2)–O(2)	90.63(8)
O(3)–Nd(1)–O(2)	79.70(4)	O(2)–Fe(2)–O(2)	89.37(8)
O(4)–Nd(1)–O(4)	54.8(2)	O(2)–Fe(2)–O(2)	180.0000
O(4)–Nd(1)–O(2)	70.56(5)	O(2)–Fe(2)–Li	24.8(2)
O(2)–Nd(1)–O(2)	135.98(6)	O(2)–Fe(2)–Li	55.2(2)
O(1)–Nd(2)–O(2)	78.25(5)	Fe(1)–O(1)–Nd(2)	180.000
O(1)–Nd(2)–O(4)	139.1(1)	Fe(2)–O(2)–Li	180.000
O(2)–Nd(2)–O(2)	156.49(8)	Fe(2)–O(2)–Nd(2)	74.5(2)
O(2)–Nd(2)–O(2)	87.62(6)	Fe(2)–O(2)–Nd(1)	171.8(1)
O(2)–Nd(2)–O(4)	72.59(8)	Nd(2)–O(2)–Nd(1)	87.91(7)
O(2)–Nd(2)–O(4)	127.39(7)	O(2)–Li–O(2)	100.25(8)
O(4)–Nd(2)–O(4)	81.8(1)	O(2)–Li–Fe(2)	83.6(3)
O(4)–Nd(2)–O(4)	55.15(8)		

Nd(2) with multiplicity 12, resulting in 36 neodymium atoms per unit cell. The oxygen atoms are located on four independent positions, i.e., O(1), O(2), O(3) and O(4). The corresponding multiplicities of the oxygen positions are 12, 48, 12, and 24, and the respective population factors are 0.749, 0.988, 0.520 and 0.558. The oxygen O(3) and O(4) are located on the faces of the cubic cell, O(1) is located along its edges and O(2) is positioned inside the unit cell.

The Fe(1) is coordinated by six O(1) oxygens forming a regular octahedra with Fe(1)–O(1) bond distances of 1.823(7) Å, while Fe(2) is also coordinated with six oxygen O(2) in the form of a regular octahedra with Fe(2)–O(2) bond distances of 2.021(2) Å as well as at longer distances. In a single unit cell the octahedra are repeated by the symmetry operations, i.e., Fe(1) is repeated twice and Fe(2) is repeated eight times.

The feature of this structure is that the lithium-containing trigonal prisms share a pair of opposite faces

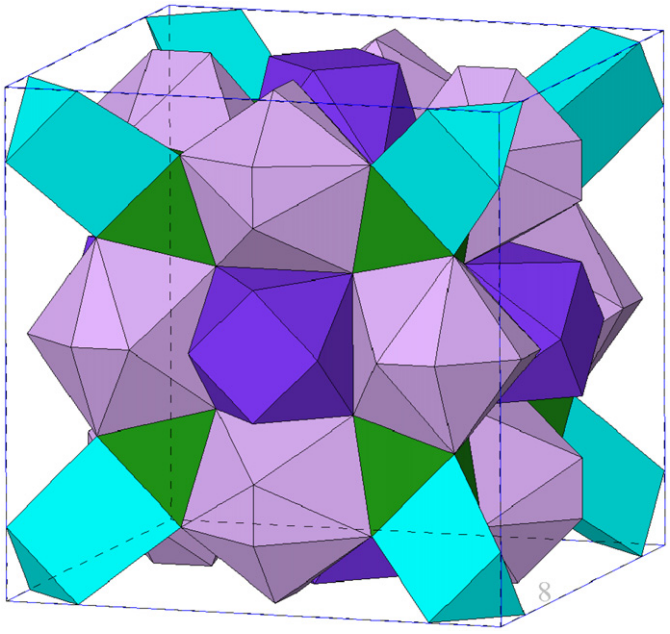

Fig. 1. Representation of the $Li_{1.746}Nd_{4.494}FeO_{9.493}$ structure. Gray/violet polyhedra contain $Nd^{3+}(1)$, dark blue polyhedra contain $Nd^{3+}(2)$, dark green octahedra contain $Fe^{3+}(2)$ and light blue trigonal prisms contain Li^{+}. The octahedra containing $Fe^{4+}(1)$ located at the corners of the unit cell are not shown.

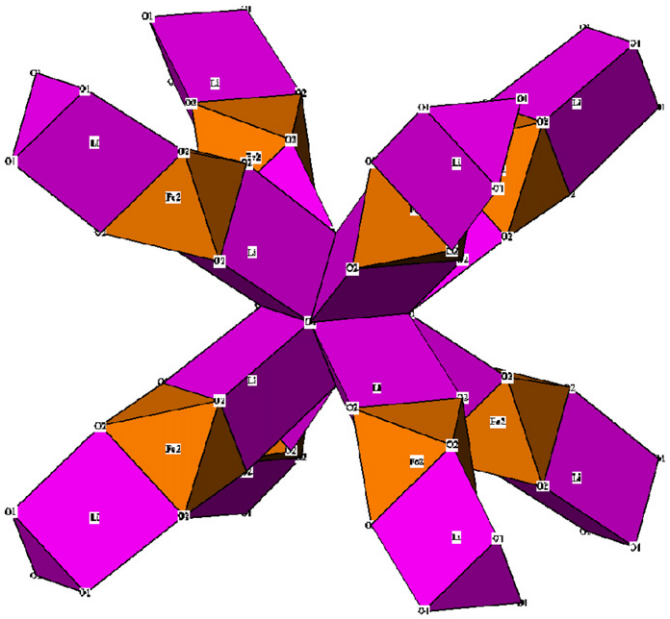

Fig. 2. Characteristic structural motif representing iron coordination octahedra Fe(1) in center and Fe(2) (orange) with corresponding lithium trigonal prisms (violet).

alternating with iron-containing octahedra along each body diagonal Figs. 1 and 2. In particular, the Fe(1) iron octahedra share all eight faces with the trigonal faces of the lithium prisms, while the Fe(2) octahedra share only two opposite faces with lithium prisms. The other six equatorial faces share with the Nd(1) polyhedra. Nd(1) has coordination 10 in the form of a dicapped square antiprism, Fig 3a, while Nd(2) has coordination nine in the form of a monocapped square anti-prism, Fig. 3b. The Nd(2) polyhedra are connected to twins by sharing the square faces.

The bond-valence sum calculated for Fe(2) using the bond-valence parameters $R(Fe^{3+})$ and $R(Fe^{4+})$ are 2.959 and 3.126, respectively. Here, when using both bond-valence parameters $R(Fe^{3+})$ and/or $R(Fe^{4+})$ the bond-valence sum is close to the expected values, so that this lattice site is most probably occupied exclusively by Fe^{3+} ions. On the other hand, the bond-valence sums calculated for Fe(1) using the bond-valence parameters $R(Fe^{3+})$ and/or $R(Fe^{4+})$ are 4.96 and 5.35, respectively. The relatively high values clearly indicate that the Fe^{4+} are located on these lattice sites. However, such a high bond-valence sum estimated for the Fe(1) lattice sites suggests a partial occupation of this lattice site by Fe^{5+}.

One of the most important features of this structure is the presence of iron in two oxidation states located on the same equivalent lattice sites, i.e., Fe^{4+} and/or Fe^{5+} on Fe(1) and the lower oxidation state Fe^{3+} on Fe(2). Such a high oxidation state of iron on both lattice sites is in accordance with the bond-valence sum predicted by the structural model of the crystal.

The second peculiarity that is characteristic for this structure is the relatively rare occurrence of the six-fold coordination of Li^+ by oxygens in the form of a trigonal prism. Such a coordination for lithium is not common; it was reported, for example, for the structures $LiAl_5O_8$ [11], $Li_{2.39}Ti_{3.4}O_8$ [12] and Li_2TiO_7 [13]. Here, the bond distances Li–O(2) are shorter than those of Li–O(1), indicating distortion of the oxygen coordination polyhedra around lithium in the crystal lattice. These irregularities are due to the fact that the lithium co-ordination polyhedron (trigonal prism) shares faces with two different iron-containing octahedra, Fe(1) and Fe(2), with different oxidation numbers and, consequently, different bond lengths, Figs. 1 and 2.

3.2. Mössbauer measurements

The Mössbauer measurement gives further evidence of the chemical and crystallographic investigation validity. The spectra (Fig. 4) recorded at 293 and 77 K indicate the

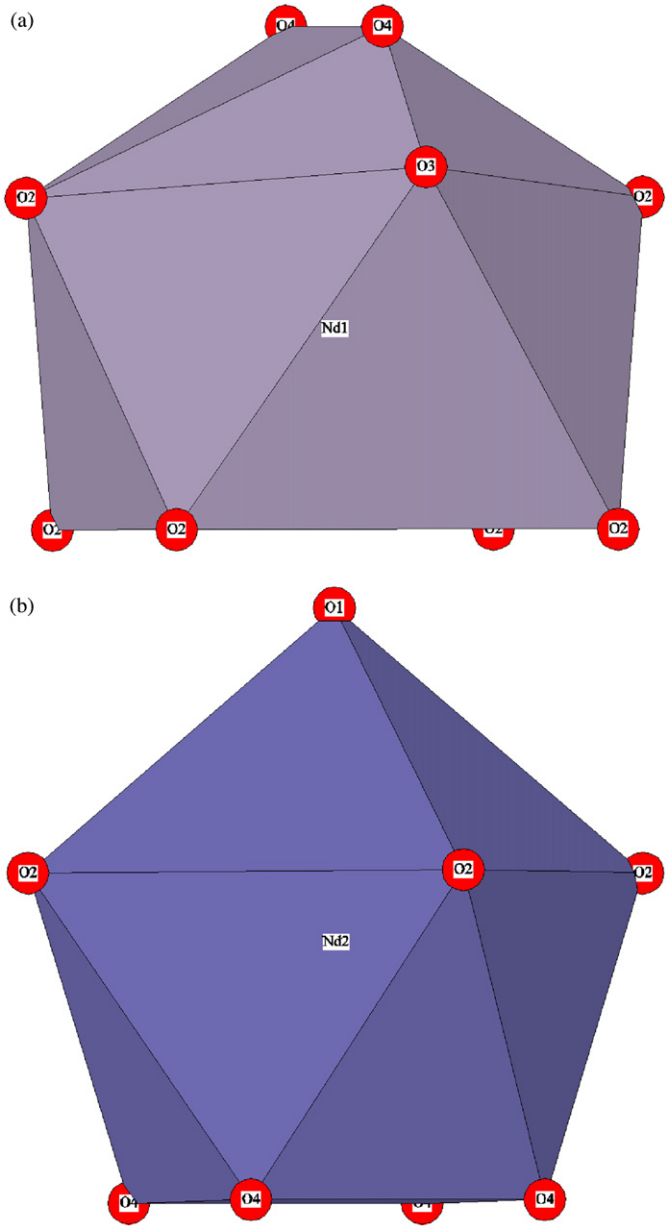

Fig. 3. Nd(1) polyhedra—coordination number 10(a) and Nd(2) polyhedra—coordination number 9(b).

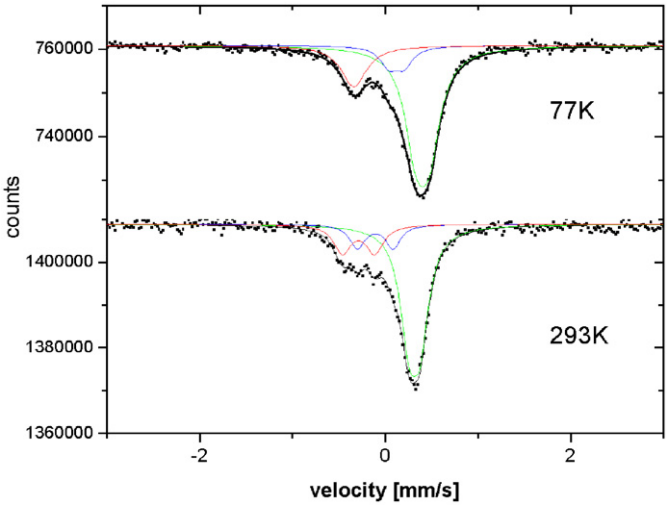

Fig. 4. Mössbauer spectra of sample $Li_{1.746}Nd_{4.494}FeO_{9.493}$ recorded at 293 and 77 K.

Table 4
Mössbauer parameters of $Li_{1.746}Nd_{4.494}FeO_{9.493}$ recorded at 293 K and 77 K, isomer shift is reported relative to metallic iron (numbers in parentheses represent errors)

Temperature (K)	Site	Isomer shift (mm/s)	Quadrupole splitting (mm/s)	Relative area (%)	Valence
293	Fe(1)	−0.108(26)	0.386(48)	14(18)	Fe^{4+}
293	Fe(1)	−0.288(28)	0.348(41)	19(13)	Fe^{5+}
293	Fe(2)	0.316(102)	0.121(15)	67.3(66)	Fe^{3+}
77	Fe(1)	0.121(53)	0.160(48)	11.1(69)	Fe^{4+}
77	Fe(1)	−0.335(15)	0.0(70)	19.3(33)	Fe^{5+}
77	Fe(2)	0.403(13)	0.143(18)	69.7(64)	Fe^{3+}

absence of magnetic behavior. The spectrum is quite complex.

Due to a cubic environment of Fe(1) and Fe(2) with a distribution of oxygen atoms the recorded Mössbauer spectra have been fitted with three quadrupole doublets with small quadrupole splittings. Fitting results are summarized in Table 4. In the room temperature spectrum the doublet with isomer shift of 0.316 mm/s has been assigned to Fe^{3+}. The quadrupole splitting is very small, i.e. 0.121 mm/s indicating a nearly cubic environment. This isomer shift value is typical of Fe^{3+} in octahedral environment [14] for Fe–O distances around 2 Å so these contribution with a spectral area of 67.3% could be assigned to Fe(2) site. The doublet with isomer shifts of −0.108 mm/s has been assigned to Fe^{4+} and doublet with isomer shift of −0.288 mm/s has been assigned to Fe^{5+}. Octahedral environments of iron with Fe–O distance smaller than 1.9 Å typically can accommodate iron atoms with valence states 4+ and higher. Therefore these two doublets representing Fe^{4+} and Fe^{5+} can be assigned to Fe(1).

The spectral areas of subspectra corresponding to Fe(1) and Fe(2) sites are close to calculated values from structural data of 75.91% and 24.09%. The spectral areas could not be equated with occupation probabilities, because the recoilless fractions for different oxidation states can be different. Typical values for recoilless fraction are between 0.3 and 0.7 at room temperature. Despite this experimental uncertainty the spectral areas give quite reasonable agreement with occupation probabilities obtained from X-ray analysis.

In the spectrum recorded at 77 K the quadrupole doublet with isomer shift of 0.403 mm/s and spectral area of 69.7% has been assigned to Fe^{3+} in Fe(2) site, while the doublet with isomer shift of 0.121 mm/s has been assigned to Fe^{4+} and doublet with isomer shift of −0.335 mm/s has been assigned to Fe^{5+}.

When using these data the following chemical formula with specified iron oxidation states distributed on Fe(1) and Fe(2) lattice sites at 293 K can be estimated, i.e. $Fe^{3+}_{0.67}Fe^{4+}_{0.19}Fe^{5+}_{0.14} \equiv Fe$ and consequently $Li_{1.746}Nd_{4.494}FeO_{9.349}$. The stoichiometry of the chemical formula when using the estimated iron oxidation numbers and occupation parameters is consistent with (close to) a charge neutral lattice.

4. Conclusions

$Li_{1.746}Nd_{4.494}FeO_{9.493}$ crystallizes with a cubic unit cell, the space group *Im*3*m*, and the lattice parameter $a = 11.9763(3)$ Å. The structure consists of a network of corner-sharing dicapped square anti-prisms of neodymium Nd(1) and coordination polyhedra of lithium in the form of a trigonal prism. In between this skeleton the neodymium Nd(2) coordination polyhedra in the form of a monocapped square anti-prism and regular octahedra of oxygen-coordinated iron are located. The Mössbauer spectra revealed the presence of Fe^{3+} ions on the Fe(2) site and Fe^{4+}, Fe^{5+} ions on the Fe(1) site. The most important feature of the structure is the presence of iron in two oxidation states and the six-fold coordination of Li^{+} by oxygens in the form of a trigonal prism.

Acknowledgments

The support by the Ministry of Higher Education, Science and Technology of the Republic of Slovenia within the National Research Program is gratefully acknowledged. The authors would also like to thank Dr. Bojan Budič from National Institute of Chemistry, Slovenia for the chemical analysis.

References

[1] I. Ban, M. Drofenik, D. Suvorov, D. Makovec, Mater. Res. Bull. 40 (2005) 1856.
[2] D. Mazza, F. Abatista, M. Vallino, J. Less. Comm. Metals 106 (1985) 277.
[3] F. Abbattista, D. Mazza, M. Vallino, M. Gazzano, J. Less. Comm. Metals 142 (1988) 203.
[4] F. Abbattista, D. Mazza, M. Vallino, M. Gazzano, J. Less. Comm. Metals 144 (1988) 311.
[5] M. Montrosi, D. Mazza, E.M. Vallino, Chim. Generale Inorgan. 122 (1988) 3.
[6] N.E. Brese, M. O'Keeffe, Acta Cryst. B 47 (1991) 192.
[7] I.D. Brown, D. Altermatt, Acta Cryst. B 41 (1985) 244.
[8] F.R. Ahmed, S.R. Hall, C.P. Huber (Eds.), Crystal Structures, Crystallographic Computing, Munksgaard, Kobenhavn, 1970 p. 292.

[9] S.R. Hall, G.S.D. King, J.M. Stewart, The Xtal3.4 User's Manual, University of Western Australia, Lamb, Perth, 1995.
[10] E. Dowty, ATOMS (V6.1) Shape software, Kingsport, USA, 2002.
[11] E. Gray, C. Li, T. Nasse, J. Sol. State Chem. 141 (1998) 222.
[12] R. Famery, F. Queyroux, J.C. Gilles, P. Herpin, J. Sol. State Chem. 30 (1979) 257.
[13] I. Abrams, P.G. Bruce, W.I.F. David, A.R. West, J. Sol. State Chem. 78 (1989) 170.
[14] F. Menil, J. Phys. Chem. Solids 46 (1985) 763.